

A Latchable Phase-Change Microvalve With Integrated Heaters

Bozhi Yang and Qiao Lin

Abstract—This paper presents a latchable phase-change microvalve with integrated microheaters, which is suitable for lab-on-a-chip systems where minimal energy consumption is desired. The microvalve exploits low-melting-point paraffin wax, whose solid–liquid phase changes allow switching of fluid flow through deformable microchannel ceiling. Switching is initiated by melting of paraffin through an integrated microheater, with an additional pneumatic pressure used for the open-to-close switching. The valve consumes energy only during initiation of valve switching. When paraffin solidifies, the switched state is maintained passively. The microvalve was fabricated from polydimethylsiloxane through multilayer soft lithography techniques. Experiments show that the valve can switch flow within 4–8 s due to the small thermal mass and localized melting of paraffin wax; when closed, the valve can passively withstand an inlet pressure over 50 kPa without leakage. Time response of the valve can be further improved with improved heater and wax chamber designs, while the latching ability can be improved by optimizing the wax chamber/membrane design. Compared to existing latchable phase-change valves, the microvalve has no risk of cross-contamination. In addition, the improved sealing offered by the compliant membrane makes the valve robust and flexible in operation, allowing large ranges of initiation pressure from various actuation schemes. [2008-0303]

Index Terms—Actuators, fluid flow control, paraffin wax, phase change, valve.

I. INTRODUCTION

MICROVALVES, which are important flow control components in microfluidic chips, generally include passive (or check) valves and active valves [1], [2]. Check valves are typically used to achieve unidirectional flow without requiring actuation. Active valves, in general, enable more versatile fluid handling, but require actuation to open and shut off fluid flow. Actuation generally requires continuous consumption of energy to maintain the microvalve in open or closed state. On the other hand, many practical applications, such as lab-on-a-chip systems, portable point-of-care medical systems, and drug delivery devices, would benefit from minimized power consumption [2]–[5]. It is therefore of great interest to develop active microvalves that operate in a more energy-efficient fashion.

Manuscript received December 12, 2008; revised May 21, 2009. First published July 15, 2009; current version published July 31, 2009. This work was supported in part by the National Science Foundation under Grants CBET-0693274 and DBI-0650020. Subject Editor C. H. Mastrangelo.

B. Yang is with Infinia Corporation, Kennewick, WA 99336 USA (e-mail: yangbozhi@yahoo.com).

Q. Lin is with the Department of Mechanical Engineering, Columbia University, New York, NY 10027 USA (e-mail: qlin@columbia.edu).

Color versions of one or more of the figures in this paper are available online at <http://ieeexplore.ieee.org>.

Digital Object Identifier 10.1109/JMEMS.2009.2024806

Paraffin waxes have been used in microvalves recently [6]–[14]. Existing paraffin-based microvalves mostly utilize the relatively large volume change of paraffin, as induced by a solid–liquid phase change, for actuation [6]–[11]. As such, they require a continuous supply of energy. In a departure from the common approach, a few latchable paraffin valves were more recently reported, which utilize the ability of a low-melting-point paraffin to hold its shape upon solidification [12]–[14]. These devices can maintain their latched open and latched closed states without energy consumption, which is attractive for many lab-on-a-chip applications. However, these devices are either single use [12] or have difficulties in controlling paraffin motion in that a modest excessive pressure could drive the melted wax completely into the liquid channel, leading to device failure [13], [14]. In addition, for these valves [12]–[14], the direct paraffin-liquid contact may induce contamination of fluid samples by paraffin wax during operation [12]–[14]. These limitations were addressed by a phase-change valve that is able to close and open a fluid flow repeatedly through a compliant membrane which separates a fluid channel from a paraffin chamber [15]. The valve exploits the latching ability of solid paraffin wax and only requires energy during switching of flow status [15]. The device is reusable and free of cross-contamination, and allows large ranges of initiation pressure generated from various actuation schemes. However, the device requires an external heat source and is bulky with a slow time response, and can hence be inadequate for practical lab-on-a-chip applications.

This paper presents a much improved latchable phase-change microvalve that features on-chip temperature control. The device has similar operation principle to the previous device [15]. It exploits the latching ability of solid-state paraffin wax, and energy consumption is only required during the valve switching. An integrated microheater is used for both heating and temperature sensing. Compared to our previous design [15], the device has drastically shorter response time, reducing the switching time to 4–8 s from 60 to 100 s in [15]. The device also offers an improved latching ability in allowing a higher critical pressure that a closed valve can hold against, less actuation energy consumption, and smaller physical size. Because of these attributes, the device is much better suited to practical lab-on-a-chip systems. The device design can be further improved, i.e., with faster time response and lower fluid temperature, to suit many biological applications.

II. DESIGN

As shown in Fig. 1, the microvalve consists of three layers: the top layer bears a microchamber, the middle layer contains

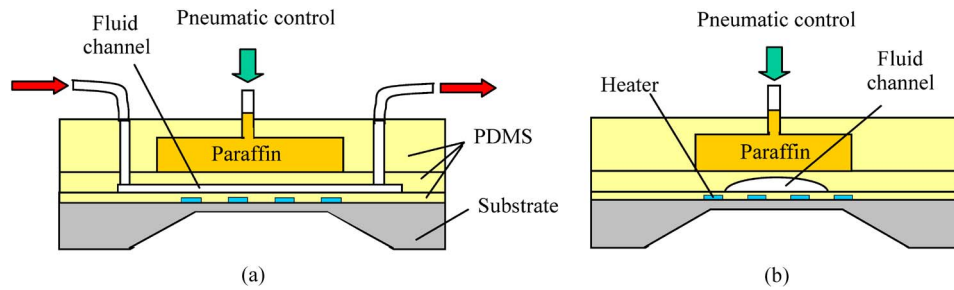


Fig. 1. Cross-sectional schematic of the phase-change microvalve. (a) Along the fluid channel. (b) Across the fluid channel. Paraffin is used as latchable phase-change actuation material. The valve closes under a pneumatic pressure and opens by the membrane’s elastic force. Both valve closure and opening require that paraffin is melted by a microheater; the open and closed states are retained passively without energy consumption after the paraffin cools and solidifies.

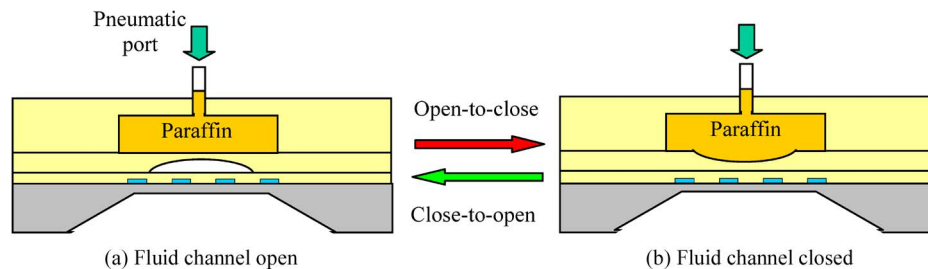


Fig. 2. Cross-sectional illustration of switching of valve states. (a) Open-to-close switching: pneumatic pressure is applied to the paraffin melted by the microheater, forcing the channel ceiling deform and shutting off the flow. (b) Close-to-open switching: upon melting of the paraffin by the microheater, channel ceiling automatically recovers to the open position under elastic force (without a pneumatic pressure).

a thin microchannel, and the bottom layer is a substrate on which a thin-film microheater is fabricated. The microchamber and microchannel are separated by a thin compliant membrane. A low-melting-point paraffin wax fills in the microchamber as the phase-change material, while the fluid flows through the microchannel. To facilitate complete closure of fluid flow, the microchannel is designed to possess a rounded cross section [Fig. 1(b)] [16]. The microchannel layer is chosen to be formed by a highly compliant material. For example, when the elastomeric polymer polydimethylsiloxane (PDMS; nominal Young’s modulus: 750 kPa [17], [18]) is used, the thin membrane between the wax chamber and fluid channel can deform readily under pressure, serving as the active valving element to allow the closing and opening of the channel to fluid flow.

When the paraffin wax is heated above the melting point, a pressure applied via the pneumatic control port of the valve can be exerted, through the molten wax, on the compliant membrane, which will deform to result in a narrowed fluid passage. When a critical pressure (i.e., shutoff pressure) is reached, the fluid flow can be shut off completely due to the rounded channel cross section. In its deformed state, the membrane generates an elastic force that tends to cause the membrane to recover to the undeformed position. Therefore, when the paraffin is heated to melt again, the channel will return to its original open state passively without the action of an external pressure. In the device, an integrated heater is used to heat and melt the paraffin wax, and an external pneumatic pressure source is used for the actuation. The actuation energy consumption and time response of the device can be significantly reduced by the use of the integrated heater.

The latchable phase-changing valve operates as follows. To shut off the flow, the low-melting-point paraffin is first heated to melt by the microheater. An external pneumatic pressure

is then applied to the molten paraffin, forcing the compliant membrane to deform and close the fluid channel. After the paraffin cools down and solidifies, the pneumatic pressure can be removed. The device is thus in a latched closed state without further consumption of energy. To open the valve, the paraffin is again heated to melt. The compliant membrane will return to its originally open position passively by its elastic force without any external force. That is, the pneumatic pressure is needed only for valve closure but not for valve opening. After the paraffin cools down and solidifies, the device remains in a latched open state. Because of the latching ability of paraffin, energy is required only during switching of the valve states and no energy is required to maintain the flow states after the switching is complete. In addition, physical separation of the fluid from the paraffin eliminates the risk of cross-contamination. Fig. 2 shows the switching between the two valve states.

III. FABRICATION

Multilayer soft lithography was used to fabricate the devices from PDMS [16], [19]. The process is shown schematically in Fig. 3. The master mold for the chamber layer was made by spin coating a 350- μm SU-8 2100 photoresist (MicroChem Corporation, Newton, MA) on a silicon wafer, which was lithographically patterned with a high-resolution (3600 dpi) transparency mask. The PDMS prepolymer (Sylgard 184, Dow Corning; 5 : 1 part A:B) was then cast against the master and cured at 65 $^{\circ}\text{C}$ for 3 h. The wax chamber layer was made relatively thick (~ 5.5 mm) for mechanical rigidity. The master mold for the fluid channel layer was fabricated by spin coating and patterning a 9 μm positive photoresist (Shipley SPR 220-7, Marlborough, MA) on a silicon wafer. The photoresist was baked at 120 $^{\circ}\text{C}$ for 20 min to create a rounded geometry for

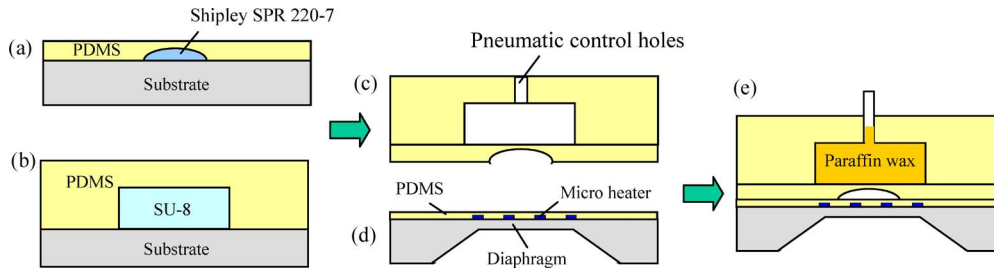


Fig. 3. Device fabrication process. (a) Spin-coating PDMS on a mold bearing reverse fluid channel features. (b) Casting PDMS on a mold bearing reverse wax chamber features. (c) Bonding the two PDMS sheets in (a) and (b). (d) Patterning microheater on substrate followed by spin coating a thin PDMS layer. (e) Bonding (c) and (d) and injecting paraffin wax.

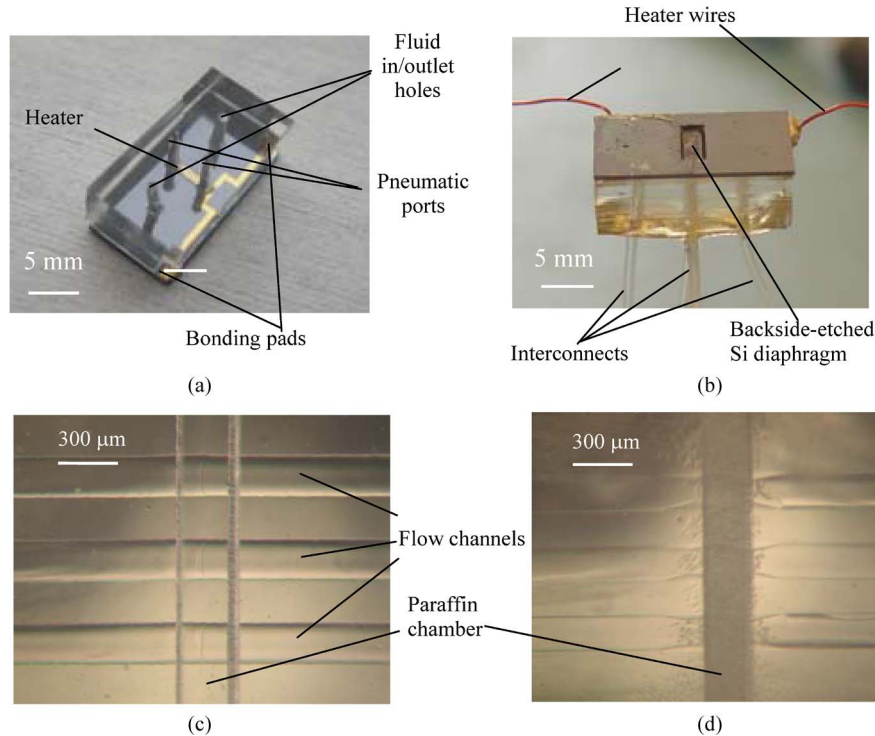


Fig. 4. Fabricated phase-change microvalve with a silicon substrate. (a), (b) Valve before and after packaging, with the front and back sides up, respectively. (c), (d) Micrographs of the fluid-containing microchannels ($200\ \mu\text{m}$ wide and $12\ \mu\text{m}$ high) and a channel poly critical dimension, paraffin-containing microchamber ($300\ \mu\text{m}$ wide and $350\ \mu\text{m}$ high) before and after paraffin filling, respectively.

the channel features to facilitate complete valve closure. The maximum channel height was measured to be about $12\ \mu\text{m}$ after the rounding. The master mold was then spin coated with PDMS (Sylgard 184; 20 : 1 part A:B) at 2500 r/min for 1 min. The resulting thin PDMS layer, about $30\ \mu\text{m}$ thick, was cured at $80\ ^\circ\text{C}$ for 30 min.

Pneumatic control holes were punched through the thick PDMS layer, which was then sealed, chamber side down, on the thin PDMS layer, aligning to the fluid channel. Bonding between the assembled layers was accomplished by curing for an additional 30 min at $80\ ^\circ\text{C}$. The resulting two-layer PDMS structure was then peeled off from the Shipley SPR 220-7 master mold (which has reverse fluid channel features), punched with the fluid inlet/outlet holes, and diced to a size of $9\ \text{mm} \times 18\ \text{mm}$.

The substrate was glass or silicon, on which integrated microheaters were fabricated. In case of silicon, the substrate was etched from the back side by Tetramethylammonium Hydroxide (with thermal oxide as an etching mask) to form a

diaphragm (approximately $100\ \mu\text{m}$ thick) for improved thermal isolation and reduced thermal mass. To fabricate the integrated microheaters, 20 nm of titanium and 250 nm of gold were E-beam evaporated and subsequently patterned on a silicon substrate or a flat glass substrate.

The diced two-layer PDMS assembly was next bonded on the diced silicon or glass substrate ($9\ \text{mm} \times 18\ \text{mm}$) covered with spin-coated PDMS (5 : 1 weight ratio of A:B at 5000 r/min; cured at $80\ ^\circ\text{C}$ for 30 min; thickness about $2\text{--}4\ \mu\text{m}$) for improved bonding strength. The entire device was then baked at $80\ ^\circ\text{C}$ overnight for complete curing of PDMS. The pneumatic control ports, fluid and electrical interconnections were finally made, and a low-melting-point paraffin wax (Sigma-Aldrich, melting point: $44\ ^\circ\text{C}\text{--}46\ ^\circ\text{C}$) was injected into the chamber in a $65\ ^\circ\text{C}$ hot water bath using a syringe. Fig. 4 shows photographs of a fabricated device with microheaters on a diaphragm formed on a backside-etched silicon substrate [Fig. 4(a) and (b)], as well as micrographs of the fluid channels and paraffin chamber before and after paraffin filling [Fig. 4(a) and (b)].

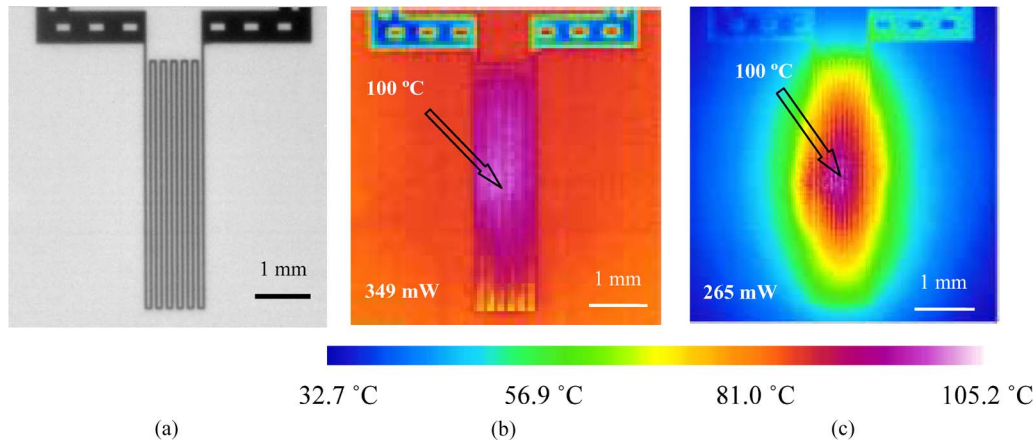


Fig. 5. IR images showing 2-D temperature distributions on the heated substrate surfaces before packaging. (a) Gray image taken by IR microscope showing microheater geometry. (b) Valve A with the heater on a freestanding silicon diaphragm (100 μm thick). (c) Valve B with the heater on the bulk of a glass substrate (700 μm thick).

IV. EXPERIMENTAL RESULTS

A. Thermal Characterization

Two latchable microvalves with integrated heaters (A and B) were tested in the experiment. Both valves included three parallel fluid channels, each having a length of 6 mm (along the flow direction), width of 200 μm (perpendicular to the flow direction), and height of 12 μm (perpendicular to the substrate plane). The wax chamber was 4 mm long (perpendicular to the fluid channels), 1 mm wide, and 350 μm high, and was located directly above the heater surface that covered the same $4 \times 1 \text{ mm}^2$ area. The two valves differed in the substrate on which the heater was fabricated. The heater of valve A [Fig. 5(a)] was fabricated on the freestanding diaphragm (5 mm long, 2 mm wide, and 100 μm thick) of a silicon substrate (500 μm thick). For valve B, on the other hand, the heater [Fig. 5(b)] was located on a flat glass substrate (700 μm thick). The measured heater resistance was 155.77 and 153.19 Ω , respectively, for valves A and B at 25 $^\circ\text{C}$.

Fig. 5 shows the steady-state temperature profile, measured via an infrared (IR) microscope (InfraScope II Micro-Thermal Imager, Quantum Focus Instruments Corporation, Vista, CA) of the two heater surfaces before packaging for valves A and B, respectively. The heaters were made to have the same maximum temperature (100 $^\circ\text{C}$) at the center by suitable choice of heating power. It can be seen that the heater on the silicon diaphragm (valve A) allowed a more uniform temperature distribution than the heater on the glass substrate (valve B). This agrees with intuition, as silicon has a much higher thermal conductivity than glass, allowing more efficient heat transfer in the substrate.

In the experiment, the integrated gold heater of each device was also used as a temperature sensor during the heating and cooling processes. The temperature sensor calibration was obtained by measuring the electric resistance of the component in an isothermal environmental chamber (Delta Design 9023) at known temperatures, as shown in Fig. 6. It can be observed that the electric resistance of each heater is a highly linear function of temperature. The temperature coefficient of resistivity (TCR), defined as the relative change of electrical resistance due to a unit temperature change, was determined to be

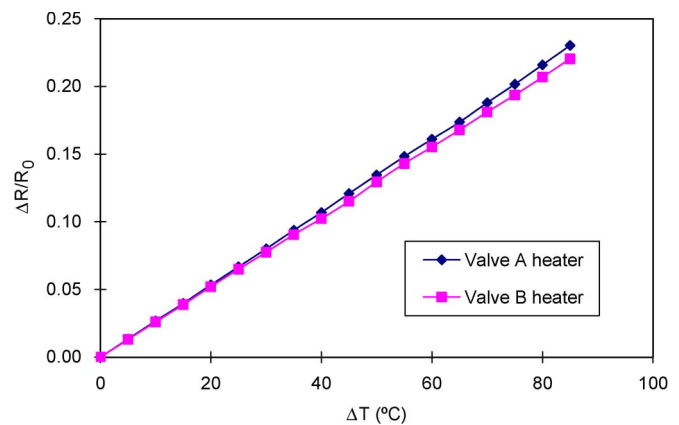


Fig. 6. Temperature dependence of electrical resistances of the gold heaters. The TCR is determined to be 0.0027/ $^\circ\text{C}$ and 0.0026/ $^\circ\text{C}$ for the heaters in valves A and B, respectively.

0.0027/ $^\circ\text{C}$ for valve A and 0.0026/ $^\circ\text{C}$ for valve B (Fig. 6). The TCR of each heater was tested four times, and the repeatability was found to be within 1%. During the valve operation, this coefficient was used to determine the temperature of the heater by measuring the resistance.

B. Microfluidic Characterization

The fabricated latchable microvalves with integrated heaters were tested with the setup shown in Fig. 7. Deionized water was used as the testing fluid and pressurized argon was used for pneumatic control during the switching of a valve from open to closed state. A digital flowmeter (Alicat Scientific L-1CCM-D, Tucson, AZ) was used to measure flow rates. Throughout the experiment, the microvalves were tested in open atmosphere at 25 $^\circ\text{C}$. To switch a valve from open to closed state, the device was heated with its integrated heater by a power of 500 mW while a 70-kPa pneumatic control pressure was applied to the paraffin. The time duration of heating required for the complete melting of the paraffin and shutoff of the flow depends on the heater design and thermal mass of the device. To switch the valve from closed to open state, it was heated again with a 500-mW power. When the wax melted, the compliant channel

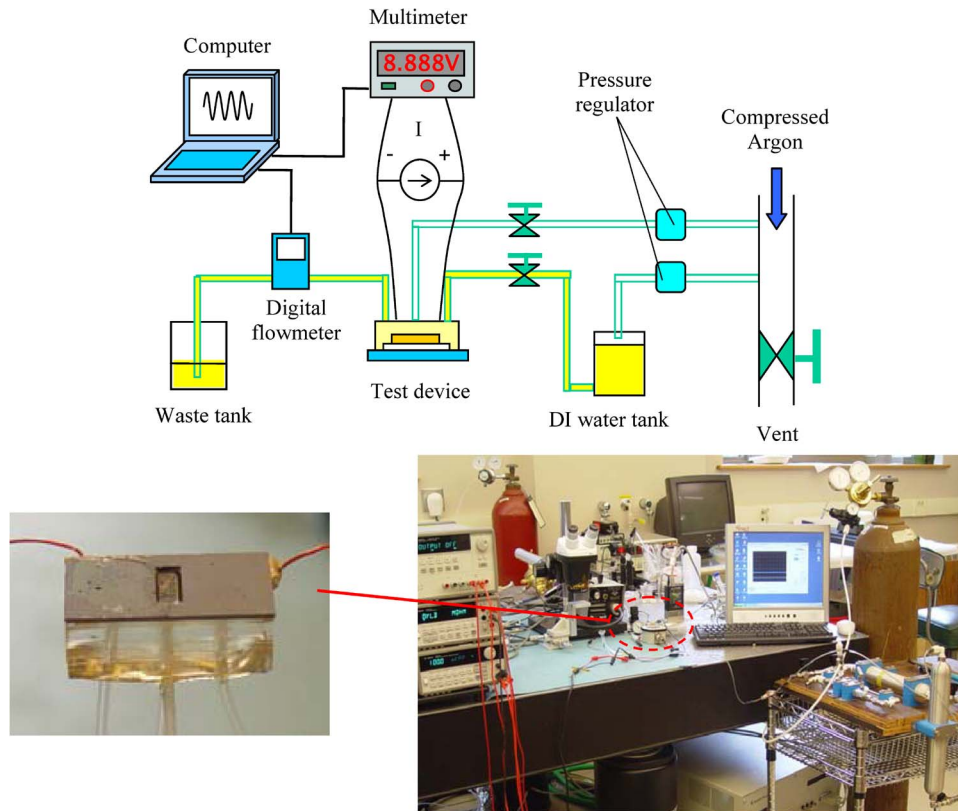


Fig. 7. Experimental setup for microfluidic characterization of the devices.

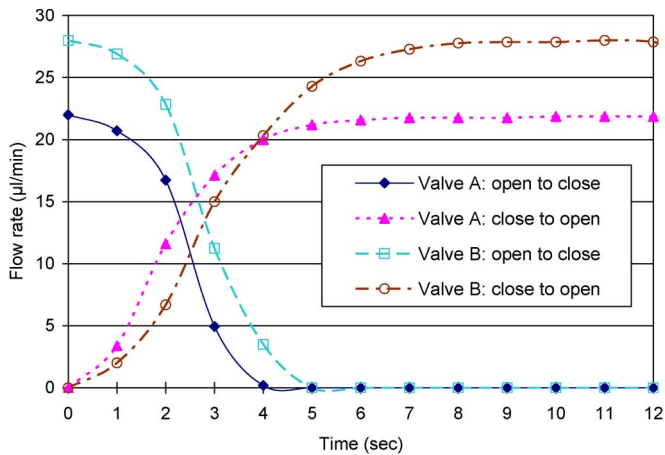


Fig. 8. Time course of valve switching between open and closed states under an inlet-outlet pressure difference of 40 kPa. The time zero corresponds to the instant at which the heating power was applied.

ceiling returned to its undeformed position under elastic force, opening the microchannels to fluid flow. Here, heating also was maintained until the valve opening was complete so that the flow rate increased to a steady value. During the heating and cooling process, the heater resistance was measured and converted to the heater temperature using the TCR. When the switching was complete, the valve would enter a latched state (in either the closed or open state) by the solidification of the paraffin as it cooled down passively.

Fig. 8 shows the measured time course of switching the valves between the open and closed states with a pressure difference of 40 kPa applied between the inlet and outlet. Each data

point in Fig. 8 represents the average of three measurements, which were repeatable with a standard deviation less than $1.85 \mu\text{L}/\text{min}$. It can be seen that the flow rates through valves A and B at the latched open states were about 22 and $28 \mu\text{L}/\text{min}$, respectively. For valve A, the open-to-close switching time was measured to be approximately 4 s, and the close-to-open switching time was about 6 s. For valve B, the open-to-close switching time was measured about 5 s and the close-to-open switching time about 8 s. The shutoff time was shorter than the opening time possibly because the pneumatic pressure applied in the testing was stronger than the passive spring force of the thin membrane. Both the closing and opening times of valve A were shorter than those of valve B. This shows that the use of a freestanding silicon diaphragm allowed valve A to have a smaller thermal mass than valve B. Therefore, one aspect of device design optimization should involve maximally reducing the device thermal mass, e.g., using thinner Si freestanding membrane, which will further reduce the device response time.

The heater temperature during the heating and cooling processes was calculated from the measured heater resistance for valves A and B. The temperature rise during the heating process, measured up to the times the valve switching is complete as shown in Fig. 7, is shown in Fig. 9. For valve A, the heater temperature rose from 25°C to 75.8°C after 4 s of heating for the open-to-close switching, and reached 84.4°C after 6 s of heating for the close-to-open switching. For valve B, the heater temperature rose from 25°C to 86.5°C after 5 s of heating for the open-to-close switching, and reached 99.1°C after 8 s of heating for the close-to-open switching.

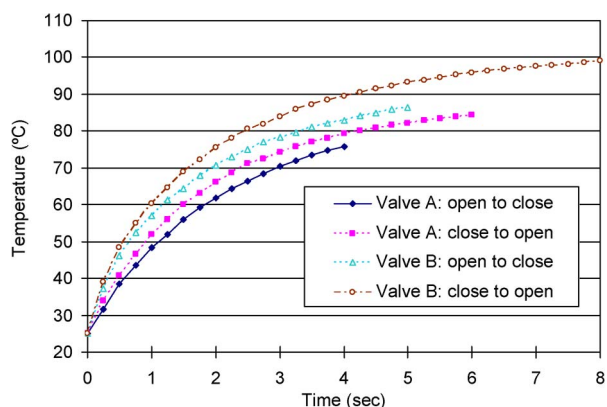


Fig. 9. Microheater temperature during paraffin melting. Measurements ended at the time (4, 6, 5, and 8 s, respectively) when the valve switching was complete.

It can also be shown from Fig. 9 that at any given time, the heater temperature for valve B was higher than that for valve A. This can be explained by the lower heat dissipation for valve B as glass has a much smaller thermal conductivity than silicon. Additionally, it can be observed that the opening and closing temperature curves do not coincide for either valve A or valve B. This may be attributed to convection heat transfer associated with the fluid flow. That is, heat dissipation was more significant, and hence the heater temperature was lower, when the fluid was in motion than when the fluid was stagnant.

These temperatures can be excessive for practical lab-on-a-chip systems, as they carry the risk of compromising certain temperature-sensitive biomolecules. However, the temperatures can be reduced by using a smaller heating power, so that the steady-state heater temperature is just slightly above the wax melting temperature (44 °C–46 °C as previously mentioned), which are, in general, not expected to cause denaturation of biomolecules such as most plasma proteins. Of course, using a smaller heating power will necessarily involve longer times needed for the wax melting and valve switching processes to complete. Therefore, there is a tradeoff to be made between the valve operation temperature and switching time. Improved designs with the heater and fluid channel on opposite sides of the wax chamber will alleviate this issue. Additionally, waxes with even lower melting temperatures (as low as 37 °C [20]) could be used to further reduce the switching temperatures.

Fig. 10 shows the time course of the heater temperature decrease during the paraffin cooling process for valves A and B. Here, the microheater was not subjected to a heating current and was used merely as a temperature sensor to monitor the cooling process. In the cooling process the valves passively cooled down in 25 °C ambient air without using a heat sink. To facilitate data comparison, the time zero in Fig. 9 is defined as the time instant when the thermally induced initiation of flow switching was completed and the heater was turned off. Therefore, the time zeros in Fig. 10 correspond to the instants at which the curves in Fig. 9 end, and are 4, 6, 5, and 8 s, respectively, after the heaters were turned on.

As can be shown from Fig. 10, it took about 8 min for valve A to cool down from 75.8 °C to 30 °C for the open-to-close

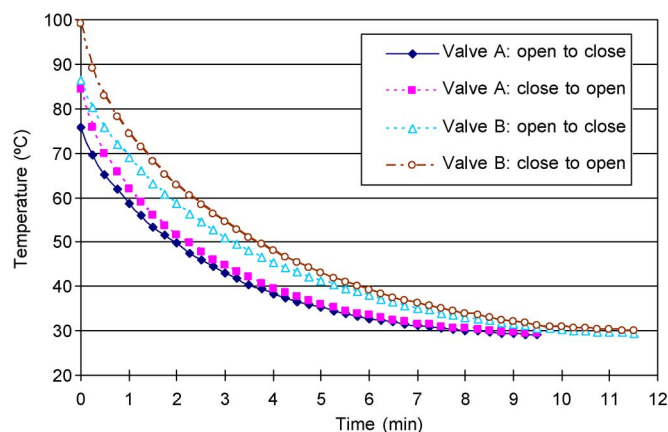


Fig. 10. Temperature of the microheater (used only as a temperature sensor) during paraffin cooling.

flow switching, and 10.25 min to cool down from 84.4 °C to 30 °C for the close-to-open switching. For valve B, it took about 8.5 min to cool down from 85.6 °C to 30 °C for the open-to-close switching, and 11 min to cool down from 99.1 °C to 30 °C for the close-to-open switching. Each curve in Figs. 9 and 10 was obtained from two to three measurements, which were repeatable with a standard deviation less than 3.5 °C.

Similar to the heating process shown in Fig. 9, Fig. 10 shows that after the cooling process started the heater temperature in valve B was always higher than that in valve A, which can be attributed to the lower heat dissipation of valve B due to the smaller thermal conductivity of glass. Valve B cooled down more slowly as it used a glass substrate. Fig. 10 also shows that for both valves A and B, the opening and closing temperature curves do not coincide. This is possibly due to convective heat transfer associated with the fluid flow in the device, i.e., heat was easier to dissipate when fluid flow was present. Therefore, the cooling period for either valve was longer for the open-to-close process than for the reverse process.

The relatively slow cooling time response of the devices can be significantly improved by exploiting forced convection or using a heat spreader, e.g., a metal plate placed underneath the actuator. The exact response time for the cooling process depends on the specific cooling conditions such as convection and heat sink properties. Note that heating and cooling time responses have different degrees of importance for practical device applications. While the heating time response is critical, a longer cooling time would only imply that the holding pneumatic pressure has to be maintained longer, which is typically not as crucial as the initiation of flow switching.

Finally, the latching capability of valves A and B was investigated. Fig. 11 shows the flow rate, measured at 25 °C, for the latched open or latched closed fluid channel subjected to increasingly large pressure differences between the inlet and outlet. Each data point in Fig. 11 represents the average of four measurements, which were repeatable with a standard deviation of 1.45 $\mu\text{L}/\text{min}$ or less. For both valves, when the valve was latched open, the flow rate was largely linear with the inlet–outlet pressure difference. This suggests that the channel cross section and flow resistance were largely constant regardless of the pressure difference. When the valve was latched

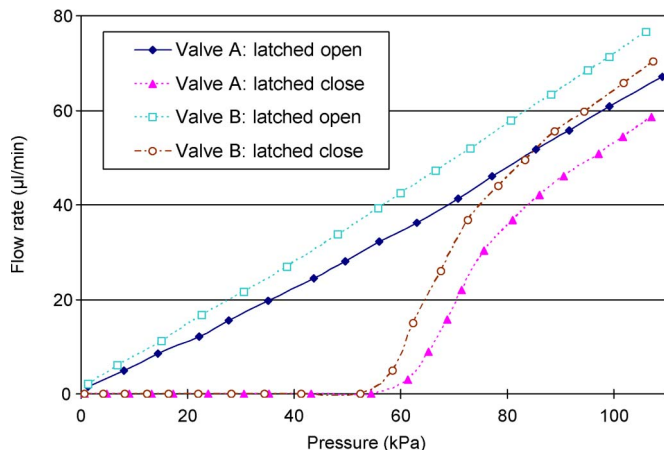


Fig. 11. Latching characteristics of valves A and B at 25 °C.

closed, the (leakage) flow rate was zero within the detection limits of the flowmeter ($1 \mu\text{L}/\text{min}$) used in the experiment, under pressure differences up to 54.5 and 52.4 kPa for valves A and B, respectively. The leakage started to increase when the pressure difference further increased as the strength of the wax became insufficient to hold the valve closed. As the pressure difference increased even further, the leakage flow rate tended to approach that obtained with the valve in latched open state. The difference between the flow rates in the two states might be caused by the inability of the compliant channel wall of the latched closed valve to completely return to its undeformed shape when the valve was latched open. The inlet–outlet pressure difference against which a valve can remain latched closed is a measure of the valve’s latching ability, which can be improved by optimal choice of membrane stiffness as well as chamber shape and dimensions.

V. CONCLUSION

A novel latchable phase-change valve with integrated heaters has been designed and characterized. The valve features a paraffin wax-filled actuation chamber separated from a fluid channel by a thin compliant membrane. Valve switching is initiated by melting of paraffin via an on-chip microheater, and after switching is completed, no energy is needed to maintain the valve state. Experiments show that the latchable valve can switch the flow within 4–8 s due to the smaller thermal mass and the localized melting of paraffin wax by the integrated heaters; and when closed, the valve can passively withstand an inlet pressure up to 50 kPa without leakage. Some advantages to the latchable phase-change valve include reusability, no risk of contamination of the fluid by paraffin wax, large ranges of initiation pressure generated from various actuation schemes. Compare to the previously reported latchable phase-change valve without integrated with on-chip heaters [15], the present valve has drastically shorter response time and a higher latching ability. It requires less thermal actuation energy for flow switching due to localized heating, is more compact in size, and is easier to be integrated with other microfluidic components. The valve is very suited for flow control in portable lab-on-a-chip systems where minimal energy consumption is desired.

The performance of the phase-change valve may be further improved. First, it would be interesting to integrate an on-chip pressure source to eliminate the usage of external pneumatic pressures. Piezoelectric, electromagnetic, and thermopneumatic actuation schemes can possibly be considered for this purpose. Second, the current integrated heater was fabricated on top of the substrate directly, and is separated from the paraffin wax by the PDMS fluid channel layer, which leads to a significant large thermal resistance. To reduce the heating time, the microheaters could alternatively be fabricated on the thin compliant PDMS layer and in direct contact with the paraffin wax. Conceptually, it is also possible to fabricate the microheaters embedded inside the paraffin chambers. Third, the shape and dimensions of the fluid channel and paraffin chamber can be optimized to improve the device’s time response and latching ability. For example, a deeper paraffin chamber may lead to higher latching ability, but it may lead to a larger thermal mass thus a slower time response. Therefore, it would be very useful to study the impact of the device geometry using finite element simulation to gain insight to the device design and operation. Finally, it is believed that the convective heat transfer associated with fluid flow may enhance heat dissipation, thus increasing the heating time and shortening the cooling time. It is believed that convection heat transfer is one of the reasons that the heating (or cooling) curve for the same device (valve A or B) differed when the same device was closed or opened. This could be investigated with coupled heat transfer and computational fluid dynamics simulations.

ACKNOWLEDGMENT

The authors would like to thank the MEMS Laboratory, Department of Electrical and Computer Engineering, Carnegie Mellon University, for generously granting access to its fabrication and characterization facilities.

REFERENCES

- [1] G. T. A. Kovacs, *Micromachined Transducers Sourcebook*. Boston, MA: McGraw-Hill, 1998.
- [2] N. T. Nguyen and S. T. Wereley, *Fundamentals and Applications of Microfluidics*. Boston, MA: Artech House, 2002.
- [3] C. Ahn, J. Choi, G. Beaucage, J. Nevin, J.-B. Lee, A. Puntambekar, and J.-Y. Lee, “Disposable smart lab on a chip for point-of-care clinical diagnostics,” *Proc. IEEE*, vol. 92, no. 1, pp. 154–173, Jan. 2004.
- [4] D. Figeys and D. Pinto, “Lab-on-a-chip: A revolution in biological and medical sciences,” *Anal. Chem.*, vol. 72, no. 9, pp. 330–335, May 2000.
- [5] F. Martin and C. Grove, “Microfabricated drug delivery systems: Concepts to improve clinical benefit,” *Biomed. Microdevices*, vol. 3, no. 2, pp. 97–108, Jun. 2001.
- [6] P. Selvaganapathy, E. T. Carlen, and C. H. Mastrangelo, “Electrothermally actuated inline microfluidic valves,” *Sens. Actuators A, Phys.*, vol. 104, no. 3, pp. 275–282, May 2003.
- [7] E. T. Carlen and C. H. Mastrangelo, “Surface micromachined paraffin-actuated microvalve,” *J. Microelectromech. Syst.*, vol. 11, no. 5, pp. 408–420, Oct. 2002.
- [8] E. T. Carlen and C. H. Mastrangelo, “Electrothermally activated paraffin microactuators,” *J. Microelectromech. Syst.*, vol. 11, no. 3, pp. 165–174, Jun. 2002.
- [9] N. Kabei, “A thermal-expansion-type microactuator with paraffin as the expansive material: Basic performance of a prototype linear actuator,” *JSME Int. J. Ser. C*, vol. 40, p. 4, 1997.
- [10] L. Klintberg, M. Svedberg, F. Nikolajeff, and G. Thornell, “Fabrication of a paraffin actuator using hot embossing of polycarbonate,” *Sens. Actuators A, Phys.*, vol. 103, no. 3, pp. 307–316, Feb. 2003.

- [11] H. J. Sant, T. Ho, and B. Gale, "A microfluidic switchboard," in *Proc. 11th Int. Conf. Miniaturized Syst. Chem. Life Sci. MicroTAS*, Paris, France, Oct. 7–11, 2007, pp. 1131–1133.
- [12] R. H. Liu, J. Bonanno, J. Yang, R. Lenigk, and P. Grodzinski, "Single-use, thermally actuated paraffin valves for microfluidic applications," *Sens. Actuators B, Chem.*, vol. 98, no. 2/3, pp. 328–336, Mar. 2004.
- [13] R. Pal, M. Yang, B. N. Johnson, D. T. Burke, and M. A. Burns, "Phase change microvalves for integrated devices," *Anal. Chem.*, vol. 76, no. 13, pp. 3740–3748, Jul. 2004.
- [14] K. W. Oh, K. Namkoong, and C. Park, "A phase change microvalve using a meltable magnetic material: Ferro-wax," in *Proc. 9th Int. Conf. Miniaturized Syst. Chem. Life Sci. MicroTAS*, Boston, MA, Oct. 9–13, 2005, pp. 554–556.
- [15] B. Yang and Q. Lin, "A latchable microvalve using phase change of paraffin wax," *Sens. Actuators A, Phys.*, vol. 134, no. 1, pp. 194–200, Feb. 2006.
- [16] M. A. Unger, H.-P. Chou, T. Thorsen, A. Scherer, and S. R. Quake, "Monolithic microfabricated valves and pumps by multilayer soft lithography," *Science*, vol. 288, no. 5463, pp. 113–116, Apr. 2000.
- [17] D. Armani, C. Liu, and N. Aluru, "Re-configurable fluid circuits by PDMS elastomer micromachining," in *Proc. 12th IEEE Int. Conf. MEMS*, Orlando, FL, Jan. 17–21, 1999, pp. 222–227.
- [18] J. Mark, *Polymer Data Handbook*. New York: Oxford Univ. Press, 1999.
- [19] B. H. Jo, L. M. V. Lerberghe, J. N. Motsegood, and D. J. Beebe, "Three-dimensional micro-channel fabrication in polydimethylsiloxane (PDMS) elastomer," *J. Microelectromech. Syst.*, vol. 9, no. 1, pp. 76–81, Mar. 2000.
- [20] Polyester Wax, EMS (Electron Microscopy Sciences) Catalog #19312, Melting point 37 °C. [Online]. Available: <http://www.emsdiasum.com/microscopy/technical/datasheet/19312.aspx> (Last accessed 2009, Jul. 1)



Kennewick, WA.

Bozhi Yang received the B.S. degree from Xi'an Jiaotong University, Xi'an, China, in 1997, the M.S. degree from Tsinghua University, Beijing, China, in 2000, and the Ph.D. degree in mechanical engineering from Carnegie Mellon University, Pittsburgh, PA, in 2006, with thesis research on creation and modeling of MEMS fluid control devices.

From 2006 to 2008, he was a Senior Engineer with the Research and Engineering Center, Whirlpool Corporation, Benton Harbor, MI. He is currently an R&D Engineer with Infinia Corporation,



Qiao Lin received the Ph.D. degree in mechanical engineering from California Institute of Technology, Pasadena, in 1998, with thesis research on robotics.

He conducted postdoctoral research on micro-electromechanical systems (MEMS) in the Caltech Micromachining Laboratory from 1998 to 2000, and was an Assistant Professor of mechanical engineering at Carnegie Mellon University, Pittsburgh, PA, from 2000 to 2005. Since 2005, he has been an Associate Professor of mechanical engineering at Columbia University, New York, NY. His research

interests are in designing and creating integrated micro/nanosystems, in particular MEMS and microfluidic systems, for biomedical applications.